Sonographic evaluation of caudal spine anomalies in children.

T P Naidich, D G McLone, A Shkolnik and S K Fernbach

AJNR Am J Neuroradiol 1983, 4 (3) 661-664
http://www.ajnr.org/content/4/3/661

Sonographic Evaluation of Caudal Spine Anomalies in Children

Thomas P. Naidich,[1] David G. McLone,[2] and Arnold Shkolnik,[1] Sandra K. Fernbach[1]

Retrospective analysis of B-mode spinal sonography in 15 pediatric patients with spinal dysraphism and caudal anomalies documents a high degree of accuracy in identifying the presence, site, size, and configuration of meningoceles; and slightly less accuracy in identifying extension of neural tissue into the meningocele and presence of concurrent lipoma. B-mode sonography is capable of displaying spinal anatomy clearly enough to permit accurate retrospective interpretation of pathologic changes. When radiologists learn to interpret sonographic images well enough to achieve equal accuracy in prospective diagnosis, then B-mode spinal sonography will supplant computed tomography and myelography as the preferred screening procedure in the initial evaluation of children with selected anomalies of the caudal spine.

Recent publications describe the anatomic derangements that characterize the diverse forms of spinal dysraphism and the syndromes of abnormal caudal regression [1, 2]. In the hope that noninvasive B-mode sonography might ultimately prove able to supplant myelography in the evaluation of some of these spinal anomalies, the authors undertook to determine the inherent limitations and optimal accuracy of spinal sonography through retrospective analysis of a series of children in whom the precise nature of the sonographic findings was documented radiologically, surgically, and pathologically.

Materials and Methods

Preoperative B-mode sonography was performed with a Rohnar 7000 scanner (North American Phillips Co.) using 3.5 and 5.0 MHz transducers in 15 pediatric patients with abnormalities of the caudal spine at The Children's Memorial Hospital, Chicago, from February 1980 through September 1982. All preoperative sonograms were analyzed retrospectively by direct correlation with patient appearance, myelography, computed tomography, surgical observation, and/or neuropathology to discern the precise nature of the structures imaged.

The 15 patients ranged in age from 1 day to 9 years. Seven patients were 3 months of age or younger. Nine patients were 1 year of age or younger. Eight were male and seven were female. The final pathological diagnoses were simple meningocele (one patient); lipomyelomeningocele (six); anterior sacral meningocele with tethered cord, lipoma, and intramedullary dermoid (one); cloacal extrophy with myelocystomeningocele (one); sacrococcygeal teratoma (one); partial sacral agenesis with hydromyelia (one); and pilonidal sinus (four). In nine cases, therefore, meningoceles formed at least one component of the lesion.

Results

Sonography documented the presence, size, site, extension(s), and exact configuration of the sometimes lobulated meningoceles in every patient with meningocele and showed direct continuity of the meningocele with the spinal subarachnoid space in every case (nine of nine). Sonography demonstrated extension or lack of extension of neural tissue into the meningocele correctly in all but one case (true-positive in seven cases, true-negative in one case, false-negative in one case). Extension of neural tissue into the anterior sacral meningocele was not demonstrated by sonography, although the presence of tethered cord and associated mass (dermoid) within the canal were documented. The roots of the cauda equina were clearly displayed in three (20%) of the 15 cases.

Highly echogenic soft tissue identified the presence of lipoma in all seven cases with lipoma, but the echogenicity of fat could not be distinguished from that of a solid sacrococcygeal teratoma in another case. In the patient with partial sacral agenesis and hydromyelia, sonography clearly defined the reduced mass of gluteal and paraspinal musculature, the absence of the sacral vertebra, substantial narrowing of the distal spinal canal, and the expanded, abnormally anechoic hydromyelic distal cord. In all four patients with pilonidal sinus, sonography clearly showed skin thickening at the dimple, deep extension of the echogenic sinus toward the coccyx, and an identifiable separation of the sinus from the normal vertebra, indicating lack of intraspinal extension of the tract.

Figures 1 through 4 illustrate a simple meningocele (fig. 1) and lipomyelomeningoceles of various sizes (figs. 2–4), permitting direct comparison of soncgrams and myelograms (and, in two cases, photographs of surgical pathology depicting the deranged spinal anatomy).

Discussion

Scheible [3] and Miller et al. [4] reported their preliminary experiences in evaluating caudal spinal anomalies using high-resolution real-time scanning and the Octoson ultrasonic scanner, respectively. In our study, articulated-arm B-mode sonography yielded

Presented in part at the annual meeting of the Society for Pediatric Radiology, Atlanta, April 1983, where it won the Caffey award.

[1]Department of Radiology, Children's Memorial Hospital and Northwestern University Medical School, 2300 Children's Plaza, Chicago, IL 60614. Address reprint requests to T. P. Naidich.

[2]Division of Pediatric Neurosurgery, Children's Memorial Hospital and Northwestern University Medical School, Chicago, IL 60614.

AJNR 4:661–664, May/June 1983 0195–6108/83/0403–0661 $00.00

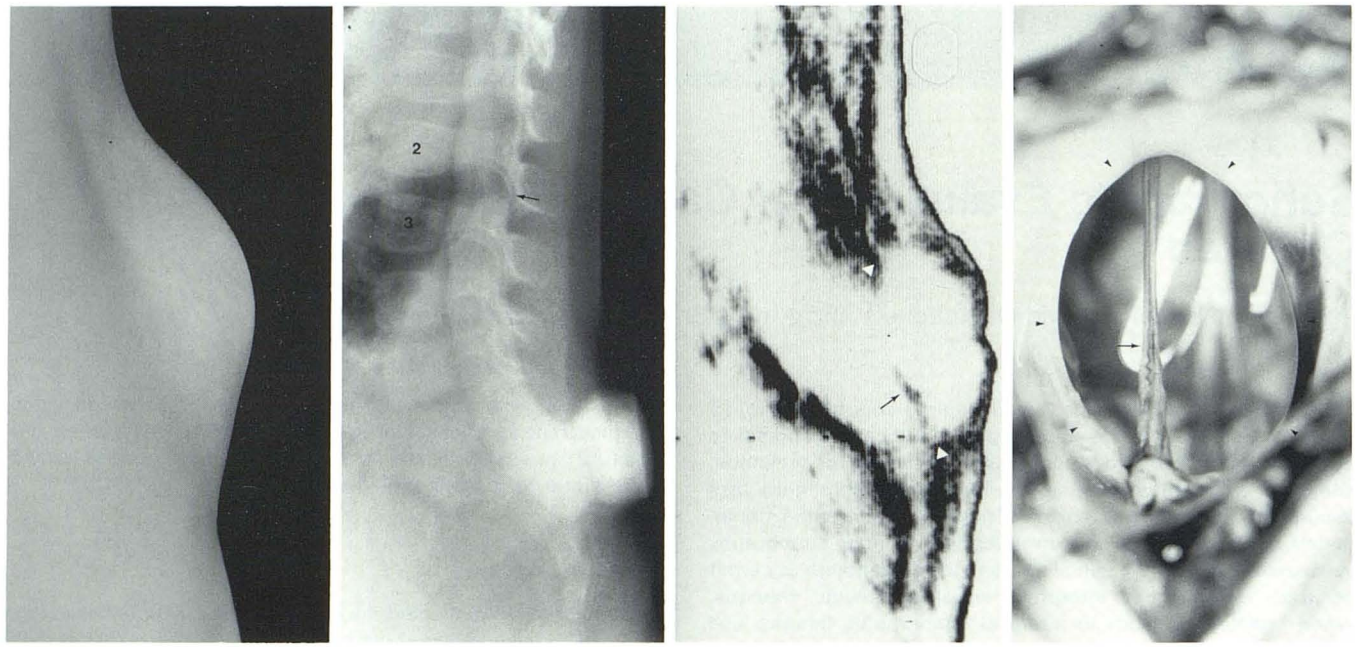

Fig. 1.—Simple meningocele, 11-month-old girl. **A**, Lateral profile of skin-covered dorsal lumbosacral mass. **B**, Lateral metrizamide myelogram demonstrates posterior meningocele, slightly low termination of spinal cord (*arrow*) within canal at L2–L3, normally descending roots of cauda equina, and absence of neural tissue or fatty mass in lesion. **C**, Midsagittal B-mode sonogram shows anechoic meningocele in direct continuity with enlarged spinal canal through relatively narrow soft-tissue and bony ostium (*arrowheads*). Thin dome of sac, absence of neural echoes in canal or sac, and absence of echogenic fat identifies simple meningocele. Linear structure (*arrow*) at lower edge of meningocele ostium is filum terminale. **D**, Surgical photograph, posterior view. Ring of tissue (*arrowheads*) marks postincision ostium of meningocele. Filum terminale (*arrow*) attaches to lower edge of ostium as in fig. 1C. White highlights are camera-flash reflections of filum terminale against cerebrospinal fluid.

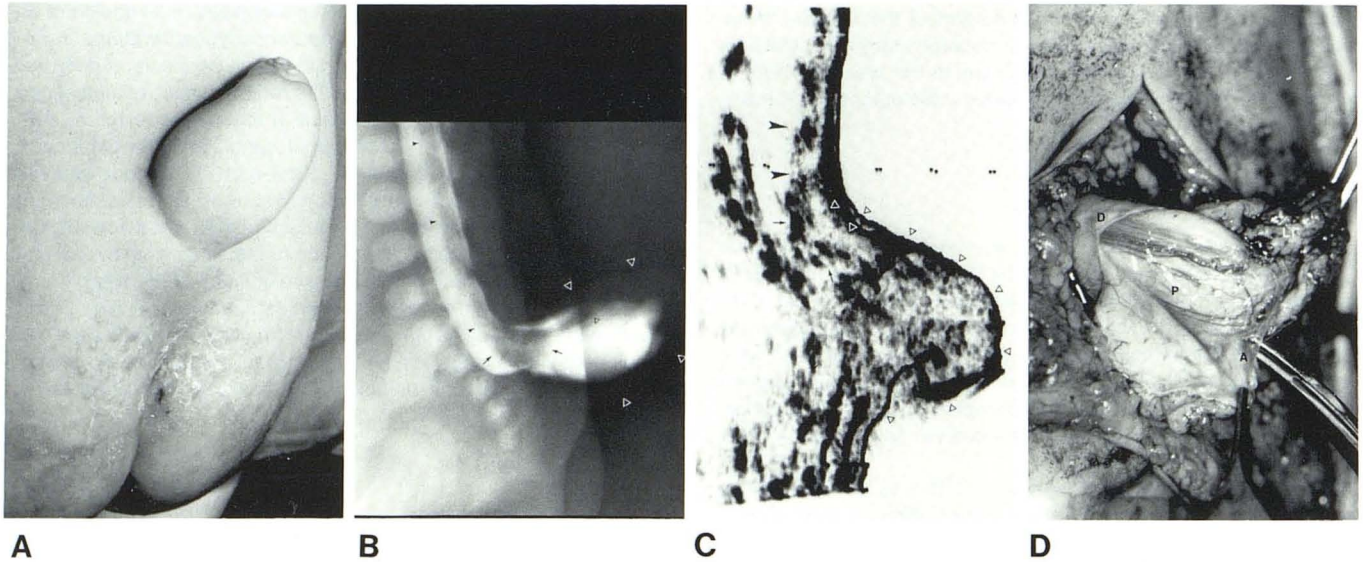

Fig. 2.—Lipomyelomeningocele, 1-month-old girl. **A**, Posterolateral view of skin-covered dorsal sacral mass. **B**, Erect lateral metrizamide myelogram demonstrates lucent mass (*open white arrowheads*) with dorsal extension of subarachnoid space and spinal cord. Cord (*closed black arrowheads*) widens inferiorly into placode (*black arrows*) as it extends through ostium. Lipoma inserts into dorsal surface of placode and continues distally as filum terminale lipoma (*open black arrowhead*). Hydrostatic pressure distends meningocele in this position. **C**, Prone, midsagittal B-mode sonogram shows echogenic lipoma (*open black arrowheads*), spinal cord (*closed black arrowheads*), widening of cord into placode (*black arrows*) at hernia ostium, and insertion of echogenic fat (*open white arrowheads*) into dorsal surface of placode. In prone position, meningeal sac has nearly collapsed and is not easily visualized. **D**, Posterolateral surgical photograph. Midline skin incision with opening of dura (D) and arachnoid (A) discloses ventral surface of placode (P) and lipoma (Li) inserting into dorsal surface of placode.

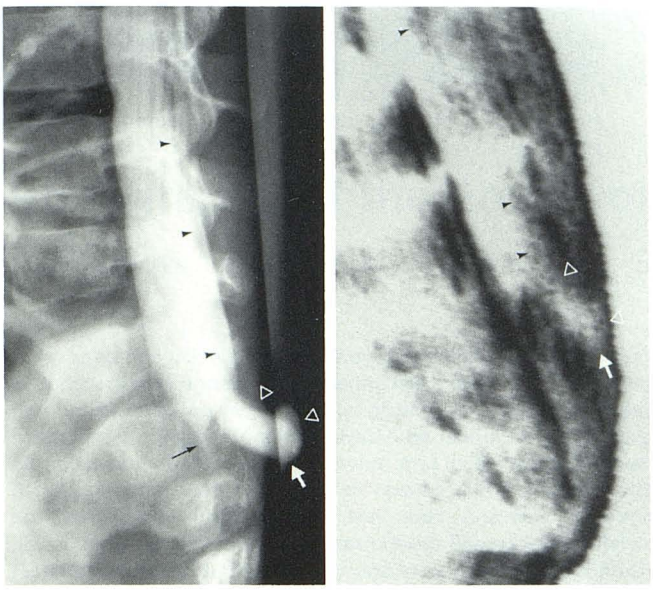

Fig. 3.—Lipomyelomeningocele, 5-year-old boy with skin-covered lumbosacral mass, naevus, and sacrococcygeal dimple. **A**, Lateral metrizamide myelogram demonstrates focal spina bifida, unusual tapering of distal sac (*black arrow*), small dorsal meningocele (*white arrow*), and tethered spinal cord (*black arrowheads*) extending along superior aspect of meningocele (*open white arrowheads*). **B**, Midsagittal B-mode sonogram also shows shape of meningocele (*white arrow*) and pointed termination of distal caudal sac. Cord tissue (*black arrowheads*) passes down spinal canal and along upper margin and dome of meningocele (*open white arrowheads*), as on myelogram. Hyperechoic fat surrounds meningocele and fills distal spinal canal, probably accounting for unusual shape of distal sac.

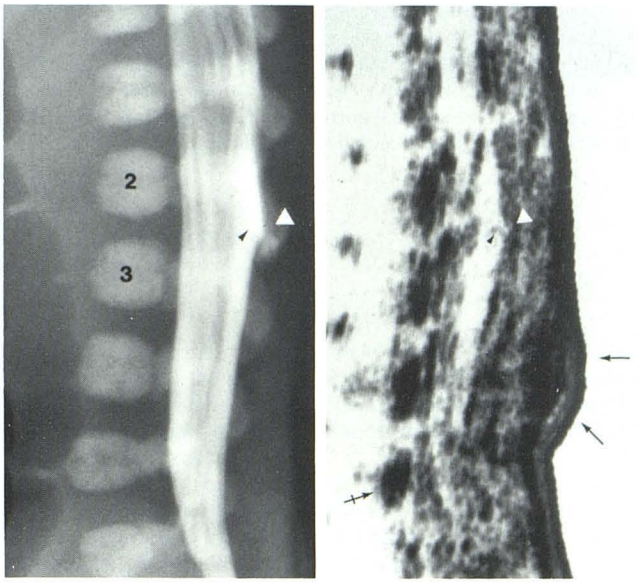

Fig. 4.—Lipomyelomeningocele, 1-month-old boy with skin-covered lumbar mass and skin tag. **A**, Lateral metrizamide myelogram demonstrates focal triangular dorsal outpouching of subarachnoid space (*white arrowhead*) at L2–L3 and faint linear strand (*black arrowhead*) extending dorsally. **B**, B-mode midsagittal sonogram shows same dorsal outpouching (*white arrowhead*) and linear strand (*black arrowhead*). Hyperechoic fat forms mass (*black arrows*) toward which meningocele and strand extend. Dorsal surface of conus and roots of cauda equina are also displayed. Most anterior vertebra (*crossed black arrow*) has posterior wall inclining posterosuperiorly, corresponding to L5 vertebra on myelogram. Triangular outpouching and strand on sonogram therefore lie opposite L2–L3 vertebra as on myelogram.

images equal in quality or superior to those illustrated by Miller et al. and achieved equal diagnostic accuracy. In our opinion, the greater length of spine included in the articulated-arm B-mode image helps in defining the interrelations of the various components of the lesion and represents a definite advantage of this technique over real-time sector scanning.

Several points on technique and interpretation are worth emphasizing:

1. Meningoceles typically distend when hydrostatic pressure is increased and become slack otherwise. For that reason, posterior meningoceles are often larger and better displayed on myelograms obtained with the patient semierect (fig. 2B) and on computed tomograms with the patient supine (but elevated off the table) than they are on routine prone sonography (fig. 2C). Patients to be evaluated for dorsal meningoceles should be studied semierect rather than supine, and should have at least some images obtained while they are crying or performing the Valsalva maneuver. In some cases with narrow ostia, sacs that were distended while the patient lay quietly have collapsed and failed to refill when the patient cried.

2. Identification of the vertebral level of a lesion displayed sonographically can be made by comparing the midsagittal sonogram with a single true lateral spine radiograph (fig. 4). One simply identifies on both studies a prominent, fixed feature such as the largest or most anterior vertebra or the apex of curvature of the fixed subcutaneous mass; determines the vertebral level of that feature on the spine radiograph; and counts the vertebrae from that point to the point of pathology.

3. The appearance of the vertebrae on transverse sonograms varies according to bone mineralization, the depth of the spine, and the thickness of the dorsal soft tissue (especially in patients with lumbar masses). For this reason, it is necessary and easy to identify the vertebrae by their shape and their relations to the usually symmetrical echogenic spinal canal and paraspinal muscle masses.

4. There are substantial limitations in B-mode sonography. The characterization of soft tissue is imprecise. Nerve roots often are not identified. Direct contact scanning cannot be performed on patients with exposed neural tissue or exposed, fragile meningeal sacs without incurring substantial risk. The technique is not always applicable to patients with repaired myelomeningoceles, because sonographic penetration of dense scar is poor.

5. Finally, the physician must undergo a significant (and perhaps discouraging) learning process before he will be able to interpret prospectively the sonographic images analyzed here retrospectively.

Nonetheless, on the basis of this study, it appears that in a substantial number of patients with caudal spine anomalies, the anatomic details of the lesions can be accurately displayed by B-mode sonography. For this reason, B-mode sonography is now the preferred initial screening procedure for evaluation of such patients at our institution.

REFERENCES

1. Naidich TP, McLone DG, Harwood-Nash DC. Dysraphism. In: Newton TH, Potts DG, eds. *Modern neuroradiology*. Vol. 1:

Computed tomography of the spine and spinal cord. San Francisco & New York: Clavadel, **1983**:299–353

2. Naidich TP, McLone DG, Mutluer S. A new understanding of dorsal dysraphism with lipoma (lipomyeloschisis): radiologic evaluation and surgical correction. *AJNR* **1983**;4:103–116
3. Scheible W. High-resolution real-time ultrasonography. In: Haller JO, Shkolnik A, eds. *Ultrasound in pediatrics. Clinics in diagnostic ultrasound*, no. 8. New York: Churchill-Livingstone, **1981**:247–263
4. Miller JH, Reid BS, Kemberling CR. Utilization of ultrasound in the evaluation of spinal dysraphism in children. *Radiology* **1982**;143:737–740